Reactivity of Molybdenum and Rhenium Hydroxo-Carbonyl Complexes toward Organic Electrophiles

Luciano Cuesta,[a] Darío C. Gerbino,[a] Eva Hevia,[a] Dolores Morales,[a] M. Elena Navarro Clemente,[a] Julio Pérez,*[a] Lucía Riera,[a] Víctor Riera,[a] Daniel Miguel,[b] Ignacio del Río,[a] and Santiago García-Granda[c]

Dedicated to Professor José Vicente on the occasion of his 60th birthday

Abstract: The hydroxo compounds [Re(OH)(CO)$_3$(N–N)] (N–N = bipy, **2a**; Me$_2$–bipy, **2b**) were prepared in a biphasic H_2O/CH_2Cl_2 medium by reaction of [Re(OTf)(CO)$_3$(N–N)] with KOH. In contrast, when anhydrous CH_2Cl_2 was used, the binuclear hydroxo-bridged compound [{Re(CO)$_3$(bipy)}$_2$(μ-OH)]OTf (**3**-OTf) was obtained. Compound [Re(OH)(CO)$_3$(Me$_2$–bipy)] (**2b**) reacted with phenyl acetate or vinyl acetate to afford [Re(OAc)(CO)$_3$(Me$_2$–bipy)] (**4**) and phenol or acetaldehyde, respectively. The reactions of [Mo(OH)(η^3-C$_3$H$_4$–Me-2)(CO)$_2$(phen)] (**1**), **2a**, and **2b** toward several unsaturated organic electrophiles were studied. The reaction of **1** with (*p*-tolyl)isocyanate afforded an adduct of *N*,*N*′-di(*p*-tolyl)urea and the carbonato-bridged compound [{Mo(η^3-C$_3$H$_4$–Me-2)(CO)$_2$(phen)}$_2$(μ-η^1(O),η^1(O)-CO$_3$)] (**5**). In contrast, the reaction of **2a** with phenylisocyanate afforded [Re(OC(O)NHPh)(CO)$_3$(bipy)] (**6**); this results from formal PhNCO insertion into the O–H bond. On the other hand, compounds [Mo[SC(O)NH(*p*-tolyl)](η^3-C$_3$H$_4$–Me-2)(CO)$_2$(phen)] (**7**), [Re[SC(O)NH(*p*-tolyl)](CO)$_3$(Me$_2$–bipy)] (**8a**), and [Re[SC(O)NHEt](CO)$_3$(Me$_2$–bipy)] (**8b**) were obtained by reaction of **1** or **2b** with the corresponding alkyl or aryl isothiocyanates. In those cases, RNCS was inserted into the M–O bond. The reactions of **1, 2a**, and **2b** with dimethylacetylenedicarboxylate (DMAD) gave the complexes [Mo[C(OH)–C(CO$_2$Me)C(CO$_2$Me)–O](η^3-C$_3$H$_4$–Me-2)(CO)(phen)] (**9**) and [Re[C(OH)C(CO$_2$Me)C(CO$_2$Me)O](CO)$_2$(N–N)] (N–N = bipy, **10a**; Me$_2$–bipy, **10b**). The molecules of these compounds contain five-membered metallacycles that are the result of coupling between the hydroxo ligand, DMAD, and one of the CO ligands. The new compounds were characterized by a combination of IR and NMR spectroscopy, and for [{Re(CO)$_3$(bipy)}$_2$(μ-OH)]BF$_4$ (**3**-BF$_4$), **4**, **5**, **6**, **7**, **8b**, **9**, and **10b**, also by means of single-crystal X-ray diffraction.

Keywords: carbonyl complexes · hydroxo complexes · insertion · molybdenum · rhenium

Introduction

Strong π-donor hydroxo, alkoxo, or amido ligands are often found in transition-metal complexes of intermediate or high oxidation states.[1] The pπ→dπ donation from OH, OR, or NR$_2$ ligands can alleviate the electron deficiency of metal centers, and thus, stabilize unsaturated species such as intermediates along dissociative pathways.[2] At the opposite extreme of ligand-bonding properties, carbon monoxide, which is ubiquitous in organometallic chemistry, requires strong dπ→pπ backbonding, and therefore, electron-rich metal centers. In spite of these disparate properties, the early belief that complexes which combine "soft" low-valent metal centers (such as classical carbonyl fragments) with "hard" OH, OR, or NR$_2$ groups would be unstable due to "soft–hard" mismatch has been disproved by thermochemical studies.[3] Actually, the electron density released from

---

[a] L. Cuesta, D. C. Gerbino, Dr. E. Hevia, Dr. D. Morales,
Dr. M. E. Navarro Clemente, Dr. J. Pérez, Dr. L. Riera,
Prof. Dr. V. Riera, Dr. I. del Río
Departamento de Química Orgánica e Inorgánica-IUQOEM
Facultad de Química, Universidad de Oviedo-CSIC
33071 Oviedo (Spain)

[b] Prof. Dr. D. Miguel
Departamento de Química Inorgánica
Facultad de Ciencias, Universidad de Valladolid
47071 Valladolid (Spain)

[c] Dr. S. García-Granda
Departamento de Química Física y Analítica
Facultad de Química, Universidad de Oviedo
33071 Oviedo (Spain)

Supporting information for this article is available on the WWW under http://www.chemeurj.org/ or from the author.

DOI: 10.1002/chem.200305577

the π-donor ligand can be transferred to the π-acceptor ligand through metal d orbitals (push–pull mechanism).[4] Therefore, the coexistence of both types of ligands on the same metal center can result in a net stabilization.

Organometallic compounds with terminal hydroxo ligands attract much interest because of their proposed participation in catalytic cycles[5] and their rich OH-centered reactivity,[6] which is dominated by the nucleophilic character of the hydroxo ligand. However, isolable examples are rare, a fact that is attributed to synthetic difficulties.[6] In truth, many hydroxo compounds have been adventitiously obtained when traces of water have been present in the reaction media.[7] On the other hand, hydroxo compounds show a strong tendency to form bi- or polynuclear species[7] in which the nucleophilicity of the OH group is decreased because it is bound to several metal atoms. This aggregation takes place when a lone electron pair of an OH group is donated into an empty coordination site of a second molecule. This can be avoided by using saturated complexes. Unfortunately, in some instances, the very π-donor character of the ligand may induce the creation of a coordination vacancy, as is the case in the *cis*-labilization of octahedral d^6 carbonyl complexes.[8] The presence of ligands with high steric bulk can be used to prevent the formation of OH-bridged species, but it can also obstruct the access of reagents to the OH functionality.

Studies on the reactivity of organometallic hydroxo complexes are scarce.[5b,9] Bergman and Woerpel reported the first reaction of an acetylene with a well characterized hydroxo complex; namely, the insertion of dimethylacetylenedicarboxylate (DMAD) into the Ir–O bond of the saturated complex $[Ir(\eta^5\text{-}C_5Me_5)(OH)Ph(PMe_3)]$.[10] Esteruelas et al. found that the unsaturated compound $[OsH(OH)(P\textit{i}Pr_3)_2(CO)]$ reacted with DMAD and other electrophiles to afford the products of formal insertion into the O–H bond.[9c] These reactivity patterns are similar to those recently reported for alkoxo or amido complexes of low-valent fragments of the Group 8–10 transition metals.[1h,6,7,11] The chemistry of hydroxo complexes of middle (Groups 6 and 7) transition-metal fragments remains virtually unexplored.

We have recently found that the saturated (18-electron) alkoxo complexes $[Mo(OR)(\eta^3\text{-allyl})(CO)_2(N\text{–}N)]$ and $[Re(OR)(CO)_3(N\text{–}N)]$ (N–N = 2,2′-bipyridine (bipy) or 1,10-phenanthroline) are easily prepared and undergo the insertion of several unsaturated organic electrophiles into the M–O bond.[12] The $[Mo(\eta^3\text{-allyl})(CO)_2(N\text{–}N)]$ and $[Re(CO)_3(N\text{–}N)]$ fragments in these complexes are reluctant to undergo ligand dissociation processes, a feature that makes them suitable for use in studies into the reactivity of the remaining position. The saturated character and robustness of these fragments would also help to prevent aggregation. Moreover, the electronic (strongly electron-releasing) and steric (planarity and lack of bulky substituents) characteristics of the N–N chelates should contribute to a high reactivity, whereas the presence of the strong π-acceptor CO ligands makes the complexes thermally stable. These ideas, as well as the paucity of previous studies in this area prompted us to explore the reactivity of the hydroxo complexes $[Mo(OH)(\eta^3\text{-allyl})(CO)_2(phen)]$ and $[Re(OH)(CO)_3(N\text{–}N)]$, the results of which we now wish to report.[13]

Results and Discussion

Synthesis of the hydroxo compounds: We recently found that the hydroxo complex $[Mo(OH)(\eta^3\text{-}C_3H_4\text{–}Me\text{-}2)(CO)_2(phen)]$ (**1**) can be conveniently prepared by reaction of $[MoCl(\eta^3\text{-allyl})(CO)_2(phen)]$ with KOH in a biphasic CH_2Cl_2/H_2O system.[14] The same conditions allowed the preparation of $[Re(OH)(CO)_3(N\text{–}N)]$ (N–N = bipy, **2a**; 4,4′-dimethyl-2,2′-bipyridine, Me_2–bipy, **2b**) complexes from triflato precursors.[15,16] In contrast, the binuclear hydroxo-bridged compound $[\{Re(CO)_3(bipy)\}_2(\mu\text{-OH})]OTf$ (**3**-OTf) was obtained (Scheme 1) after 12 h when anhydrous CH_2Cl_2 was used.[17] Each kind of complex (mono- or bimetallic) is obtained as a single product. Therefore, the presence or absence of water in the reaction medium provides a clear-cut synthetic method towards each complex, and alleviates the need for any separation steps.[18]

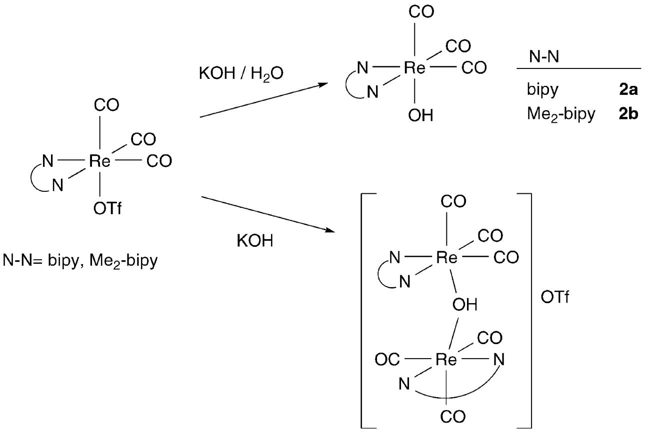

3-OTf (N-N= bipy)

Scheme 1. The mononuclear hydroxo complexes **2a** and **2b** were obtained in the presence of water, whereas the binuclear complex **3**-OTf was formed in anhydrous CH_2Cl_2.

The mononuclear complexes **2a** and **2b** display IR and ^1H NMR spectra that are comparable to those reported by Gibson et al.[16] In the solid state, the presence of the OH group in **3**-OTf gives rise to a weak, but sharp IR band at 3645 cm^{-1}. In solution, the presence of the OH ligand is indicated by a broad, one-hydrogen signal at $\delta = -1.62$ ppm in the ^1H NMR spectrum. Since our attempts to grow single crystals of **3**-OTf suitable for X-ray diffraction were unsuccessful, we prepared the analogous tetrafluoroborate derivative by reaction of **2a** with a hemimolar amount of tetrafluoroboric acid in CH_2Cl_2 (Scheme 2).[19] Crystals of **3**-BF_4, which were obtained by slow diffusion of hexane into a saturated solution of the hydroxo compound in CH_2Cl_2, were employed for a structure determination by means of X-ray diffraction. A thermal ellipsoid (30 % probability) plot of the cation is displayed in Figure 1.[20]

The cation consists of two $[Re(CO)_3(bipy)]$ fragments linked by a single hydroxo bridge. The two $[Re(CO)_3(bipy)]$ fragments are staggered in the solid-state structure, and therefore, are inequivalent. However, the NMR data for

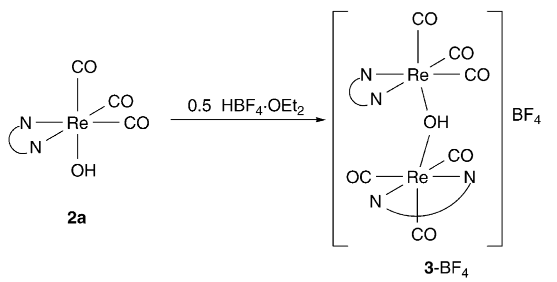

Scheme 2. Protonation of the hydroxo complex **2a** with a hemimolar amount of tetrafluoroboric acid afforded the binuclear hydroxo complex **3**-BF_4.

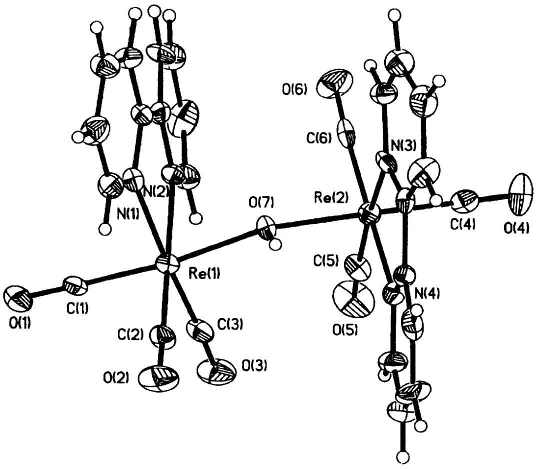

Figure 1. Thermal ellipsoid (30%) plot of the cation of **3**.

compound **3**-BF_4 in solution (see Experimental Section) indicates the presence of two apparent mirror planes that make the two metal fragments and the two halves of each bipy ligand equivalent. This is consistent with free rotation around the Re–O bonds. Such a process is expected to have a low kinetic barrier since $p\pi \rightarrow d\pi$ donation is not possible for these 18-electron fragments, and steric hindrance for such rotation is not an issue. Failure of **3**-OTf or **3**-BF_4 to react with Lewis bases or unsaturated organic electrophiles that undergo reactions with mononuclear hydroxo complexes (see below), indicates that Re–O rapid-bond cleavage and subsequent reformation is not an alternative dynamic process which would also explain the aforementioned equivalence observed in the NMR spectra.

Hydroxo ligands can act as bridges between two or more metal centers. Indeed, most structurally characterized hydroxo complexes are polynuclear species.[7] However, binuclear complexes with a single OH ligand as the only bridge are quite rare. An example is the cationic complex $[\{Mo(\mu^3\text{-methallyl})(CO)_2(phen)\}_2(\mu\text{-}OH)]^+$.[14] Most hydroxo-bridged complexes possess either several OH bridges or additional bridging groups.[21–23] The Re-O-Re angle in **3**-BF_4 (140.5(7)°) is similar to that found in the above-mentioned molybdenum complex (145.3(4)°). As expected, these values are considerably higher than those found in complexes that have several bridges.[24]

The binuclear cation present in **3**-BF_4 can be considered as an adduct between the Lewis acidic 16-electron fragment $[Re(CO)_3(bipy)]^+$ and the Lewis basic (through a lone OH electron pair) $[Re(OH)(CO)_3(bipy)]$ (**2a**; Figure 2).

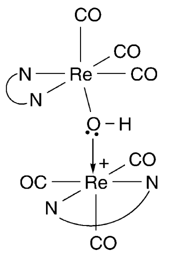

Figure 2.

We have recently isolated several adducts that contain the $[Re(CO)_3(bipy)]^+$ fragment and weakly Lewis basic molecules such as ketones, ethers, methanol, and the like.[25] Unlike these complexes, **3** is not labile. For instance, it is unreactive towards PMe_3 or pyridine. This is the case because the hydroxo-bridged complex **3** is stabilized with regard to the aforementioned labile species by delocalization of the Re–O bonds (i.e. it can be described by two equivalent resonance forms, one of which is represented in Figure 2).

One of the earliest reports of a transition-metal complex that contains single hydroxo bridges is that of $[\{Fe(OEP)\}_2(\mu\text{-}OH)]^+$ (OEP = octaethylporphyrinate). It is proposed that the μ-OH group is stabilized because it is located in a hydrophobic environment between the two OEP planes.[26] A similar disposition of the OH bridge between the two eclipsed phenanthroline planes was found in $[\{Mo(\eta^3\text{-methallyl})(CO)_2(phen)\}_2(\mu\text{-}OH)]^+$,[14] but in **3**-$BF_4$, which has staggered bipy ligands, this feature is absent. The presence of an additional ring in the phenanthroline example could lead to a greater π-stacking stabilization, and may account for this difference.

Reactivity of the hydroxo complexes $[Mo(OH)(\eta^3\text{-}C_3H_4\text{–}Me\text{-}2)(CO)_2(phen)]$ and $[Re(OH)(CO)_3(N\text{–}N)]$

Reaction of 2b with acetates: We sought to estimate the relative reactivity of $[Mo(OH)(\eta^3\text{-}C_3H_4\text{–}Me\text{-}2)(CO)_2(phen)]$ (**1**) and $[Re(OH)(CO)_3(N\text{–}N)]$ (**2a** and **2b**), in comparison to previously known monometallic saturated hydroxo compounds, towards electrophiles. Bergman et al. reported that $[Ir(\eta^5\text{-}C_5Me_5)(OH)Ph(PMe_3)]$ reacts with phenyl acetate to give a mixture of the phenoxide and acetate complexes after 36 h at 60 °C.[6] ^1H NMR monitoring showed that the reaction of $[Re(OH)(CO)_3(Me_2\text{–}bipy)]$ (**2b**) with PhOAc in CD_2Cl_2 afforded $[Re(OAc)(CO)_3(Me_2\text{–}bipy)]$ (**4**) (see Scheme 3a) and phenol as the only products, and was complete in 20 h at room temperature. The analogous reaction with **1** was complete within 8 h; this indicates that the molybdenum complex has a higher reactivity. In a separate experiment, the reaction was conducted in CH_2Cl_2 on a preparative scale. Compound **4** was isolated in high yield, and was characterized by IR and NMR spectroscopy (see Experimental

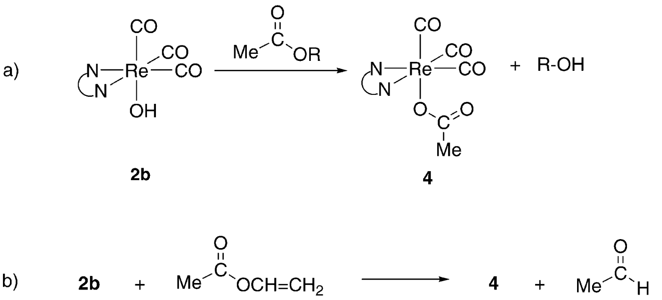

Scheme 3. Reaction of **2b** with acetates.

Section), as well as by X-ray diffraction (Figure 3). Complex **2b** also reacted with vinyl acetate to afford **4** and acetaldehyde (the stable tautomer of the expected vinyl alcohol) (Scheme 3b). These results encouraged us to study the reactivity of the molybdenum and rhenium hydroxo complexes **1**, **2a**, and **2b** with different organic electrophiles.

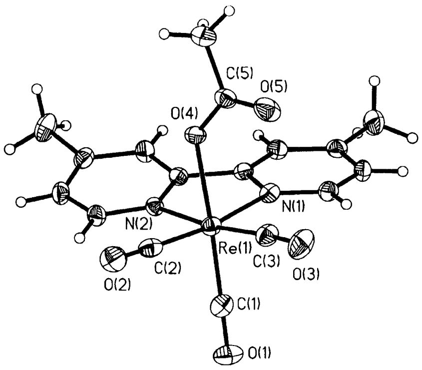

Figure 3. Thermal ellipsoid (30%) plot of complex **4**.

Reactions with arylisocyanates:[27] As indicated by the shift to higher wavenumber values of the two similarly intense ν_{CO} IR bands, which is diagnostic of the persistence of a *cis*-$Mo(CO)_2$ unit, complex [Mo(OH)(η^3-C_3H_4–Me-2)$(CO)_2$(phen)] (**1**) reacted instantly with a stoichiometric amount of (*p*-tolyl)NCO. The presence of several sets of phen signals in the ^{1}H NMR spectrum of the crude solid, which was obtained by evaporation of the solvent, indicated the presence of several products. The major compound was isolated by two successive crystallizations and was found to consist of an adduct of *N,N'*-di(*p*-tolyl)urea and the carbonato-bridged complex [{Mo(η^3-C_3H_4–Me-2)$(CO)_2$(phen)}$_2$(μ-η^1,η^1-CO_3)] (**5**) (see Scheme 4). An IR band at 1516 cm^{-1} was assigned to the stretching mode of the carbonato bridge.[28]

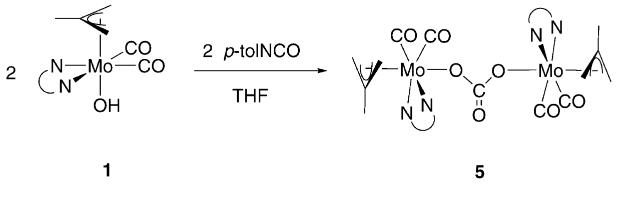

Scheme 4. Reaction of **1** with *p*-tolNCO afforded an adduct of the carbonate-bridged complex **5** and *N,N'*-di(*p*-tolyl)urea.

The solid-state structure of **5**·*N,N'*-di(*p*-tolyl)urea was determined by X-ray diffraction, and the results are displayed in Figure 4.[20]

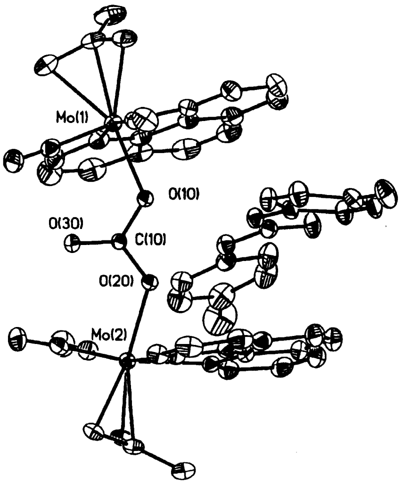

Figure 4. Thermal ellipsoid plot at the 30% probability level for the adduct **5**·*N,N'*-di(*p*-tolyl)urea.

The ^{1}H NMR spectrum of **5** exhibits only four phen signals and three methallyl signals. This indicates the existence of an apparent mirror plane that makes the two [Mo(η^3-C_3H_4–Me-2)$(CO)_2$(phen)] fragments and the two halves of each of these fragments equivalent. This symmetry is further supported by the ^{13}C NMR data. In view of the structure of **5** in the solid state (Figure 4), even if these mirror planes were absent, the apparent symmetry observed in the spectra could be attributed to free rotation around the Mo–O bonds. The Mo–O distances (2.126(3) and 2.157(3) Å) are consistent with single bonds;[29] this indicates that both molybdenum atoms have 18-electron configurations. In structure **5**, the [Mo(η^3-C_3H_4–Me-2)$(CO)_2$(phen)] fragments are unremarkable. The carbonato bridge is planar at carbon (sum of angles about C(10) = 360°) and the C=O (terminal) distance (1.214(5) Å) is shorter than the two C–O (bridge) values (1.314(5) and 1.329(5) Å). The molecule of *N,N'*-di(*p*-tolyl)urea is oriented so that the nitrogen-bonded hydrogens point toward the open face of the bridging OCO group. The angle between the NCN (urea) and OCO (carbonato) planes is 75°. One would expect that a coplanar geometry would provide the best N–H···O bonding interactions. However, the actual arrangement combines the N–H···O hydrogen bond (the shortest distances are N(71)–O(20) = 3.098(5) and N(72)–O(10) = 2.939(5) Å) with aryl–aryl π stacking between *p*-tolyl and the phen rings (see Figure 3b in the Supporting Information).

Several carbonato-bridged binuclear transition-metal complexes are known, and most of them featuress η^1(O),η^1(O) bridges like that present in **5**.[30] In some instances, these species arise from reactions of hydroxo complexes with CO_2.[9d,30b,31] Initially, a hydrogenocarbonato (bicarbonato) complex is formed. Subsequent condensation between this compound and the hydroxo complex affords the carbonato complex. The generation of a carbonato complex in a reaction with an isocyanate is, to the best of our knowledge, unprecedented. The formation of complex **5** can be rationalized according to the mechanism depicted in Scheme 5. Initial attack by the undissociated OH group in compound **1** yields a zwitterionic intermediate. Oxygen is then displaced by nitrogen; this is driven by the higher donor character of the amido group with respect to the ether (see resonant form B in Scheme 5). The intermediary N-bound compound between A/B and C is proposed on the basis of the results found for reactions of RNCO with related Re–OMe complexes (vide infra).[12] The Mo–N product then undergoes a H^+ transfer from oxygen to the more basic nitrogen to give the O-bound carbamato product C (alternatively, a H^+ shift could transform A directly into C), as this favors coordination through the anionic carboxylic oxygen instead of the bulkier amino group. This mechanistic rationale is similar to the one recently proposed to explain the different products obtained from the reaction of rhenium amido complexes with isocyanates,[32] as well as products obtained from other reactions of hydroxo complexes (see below).[32,33] At this point, nucleophilic attack of the carbamate group in C by the hydroxo group in **1** affords complex **5** and free (*p*-tolyl)amine. Complex **5** then reacts with free (*p*-tolyl)NCO to give the uric product.[34] Although we have attempted to exclude water from the reaction medium, hydrolysis of the proposed carbamato intermediate C cannot be ruled out as an alternative pathway for the formation of the carbonato product.[35]

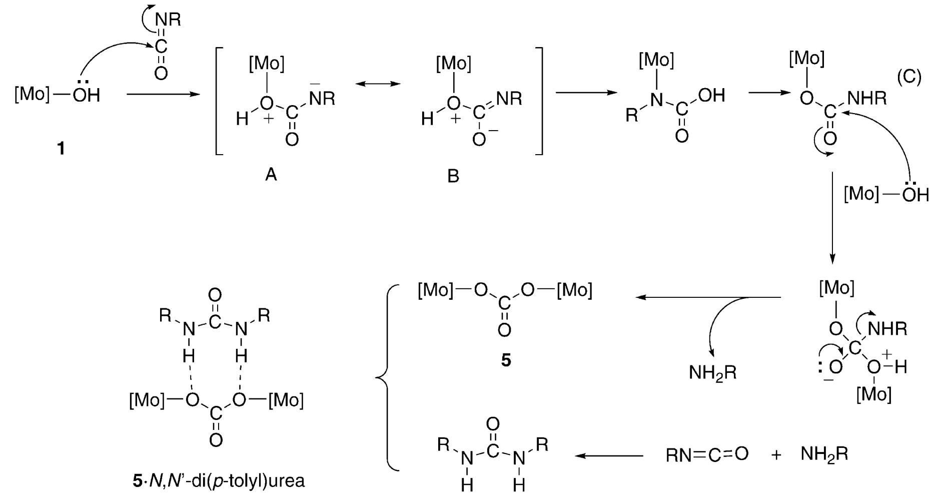

Scheme 5. Proposed mechanism for the formation of **5**·*N*,*N*'-di(*p*-tolyl)urea.

Complex $[Re(OH)(CO)_3(bipy)]$ (**2a**) reacts with phenylisocyanate to give the product from formal PhNCO insertion into the O–H bond, as shown in Scheme 6. The reaction, which is instantaneous at room temperature, is accompanied by a color change of the dichloromethane solution from orange to yellow, and an increase (as expected for a reaction with an electrophile) of some 10 cm^{-1} in the ν_{CO} IR bands. IR and ^1H NMR monitoring showed the formation of a single product, which was isolated by crystallization. The ^1H NMR spectrum showed signals for a symmetric bipyridine, which indicates the presence of a molecular mirror plane, as well as an aromatic multiplet that confirmed the incorporation of PhNCO, and a broad one-hydrogen signal at $\delta = 5.99$ ppm that could be attributed to an NH or OH group. The low solubility of the product precluded the acquisition of a significant ^{13}C NMR spectrum. Since the available data did not allow a structural assignment, the solid-state structure was determined by single-crystal X-ray diffraction. The results are shown in Figure 5[20] and indicate a $[Re(OC(O)NHPh)(CO)_3(bipy)]$ (**6**) formulation. The molecule displays a pseudo-octahedral geometry typical of $[ReX(CO)_3(N{-}N)]$ complexes, and consists of a $[Re(CO)_3(bipy)]$ fragment bonded to one of the oxygen atoms of an *N*-phenylcarbamato ligand. The Re–O bond (2.110(7) Å) is comparable to that found by Gibson et al. in the complex $[Re(OH)(CO)_3(Me_2{-}bipy)]\cdot 2.5\,H_2O$ (2.132(3) Å).[16] A lengthening of the Re–O distance in comparison with the hydroxo precursor would be expected for **6** as a result of the carbamato ligand being a poorer donor than the hydroxo ligand (as indicated by the higher ν_{CO} values for the latter). Indeed, this has been the trend found for insertion of other organic electrophiles into Re–O or Re–N bonds in related compounds.[12,32,33] The fact that this lengthening of the Re–O bond is not observed for **6** with respect to the hydroxo complex can be attributed to hydrogen-bond interactions of the OH ligand with water molecules in the latter complex; this can weaken the Re–OH

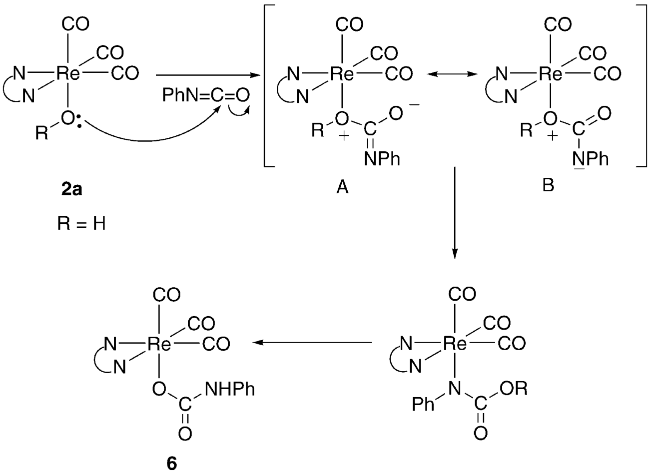

Scheme 6. Reaction of **2a** with PhNCO afforded complex **6**, which contains a monodentate *N*-phenylcarbamato ligand.

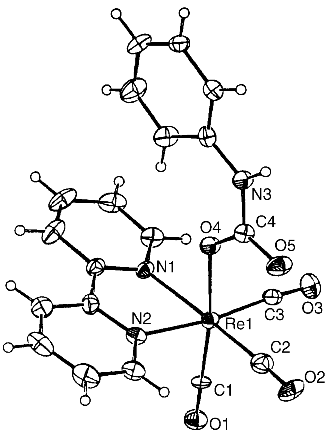

Figure 5. Thermal ellipsoid (30 % probability level) plot of **6**.

bond and increase the Re–OH distance.[36] Thus, the Re–O distance in $[Re(OMe)(CO)_3(bipy)]$ is 2.081(5) Å.[37] A similar or perhaps even shorter distance could be expected for an Re–OH bond in the absence of such interactions given the smaller size of the OH group in comparison to an OMe group.[38] The distances for the C(4)–O(5) (1.246(9) Å) and C(4)–N(3) (1.400(10) Å) bonds are consistent with double and single bonds, respectively.[39] Moreover, the sum of the angles around C(4) is 360°; this indicates an sp^2 hybridization, and that the metrical data support the formulation shown in Scheme 6. Scheme 6 is a mechanistic proposal that allows us to rationalize not only the results presented here, but also previous related ones, such as reactions of isocyanates with Re–OMe compounds. However, simpler alternatives do exist. For instance, H^+ transposition from O to N would explain the direct transformation of A into B.

The reaction of a transition-metal hydroxo complex with an isocyanate has, to the best of our knowledge, only recently been reported by Esteruelas et al. The unsaturated, five-coordinate osmium hydroxo complex $[OsH(OH)(CO)(PiPr_3)_2]$ reacted with PhNCO to give the product from formal isocyanate insertion into the O–H bond.[9c] A major difference with respect to complex **5** is that the osmium product features a bidentate carbamato ligand. The formation of a monodentate carbamato linkage in our rhenium complex is enforced by the saturated nature of the rhenium fragment, and is also the reason why reactions of isocyanates, isothiocyanates, and carbon disulfide with alkoxo and amido complexes leads to the formation of monodentate ligands.[12,32,33,40]

Reactions with isothiocyanates: Complex **1** reacts with (*p*-tolyl)NCS, while **2b** reacts with (*p*-tolyl)NCS and EtNCS to afford, after 15 minutes at room temperature, $[Mo[SC(O)NH(p\text{-tolyl})](\eta^3\text{-}C_3H_4\text{–}Me\text{-}2)(CO)_2(phen)]$ (**7**), $[Re[SC(O)NH(p\text{-tolyl})](CO)_3(Me_2\text{–}bipy)]$ (**8a**), and $[Re[SC(O)NHEt](CO)_3(Me_2\text{–}bipy)]$ (**8b**), respectively. Both alkyl and aryl isothiocyanates react with molybdenum and rhenium hydroxo complexes to afford products similar to the ones described here, but for the sake of brevity we will limit our discussion to representative examples that could be fully characterized, and their structures determined by means of single crystal X-ray diffraction. Complexes **7, 8a**, and **8b** were characterized by IR, ^1H NMR, and ^{13}C NMR (for **8b**) spectroscopy, and single crystal X-ray diffraction was conducted on **7** and **8b** (Figure 6). The spectroscopic data include signals for the *p*-tolyl or ethyl group and, for complex **8**, a weak signal in the ^{13}C NMR spectrum at $\delta = 175.35$ ppm that can be attributed to the central carbon of the thiocarbamato ligand (see below). The N-bonded hydrogen atoms occur as broad signals at $\delta = 7.43$ ppm (**7**) and $\delta = 5.90$ ppm (**8a**) in the ^1H NMR spectra. For complex **8b** this signal is not observed in the ^1H NMR spectrum obtained at room temperature, but was visible at −40 °C as a broad singlet at $\delta = 5.50$ ppm. The solid-state structures of each molecule are presented in Figure 6.[20]

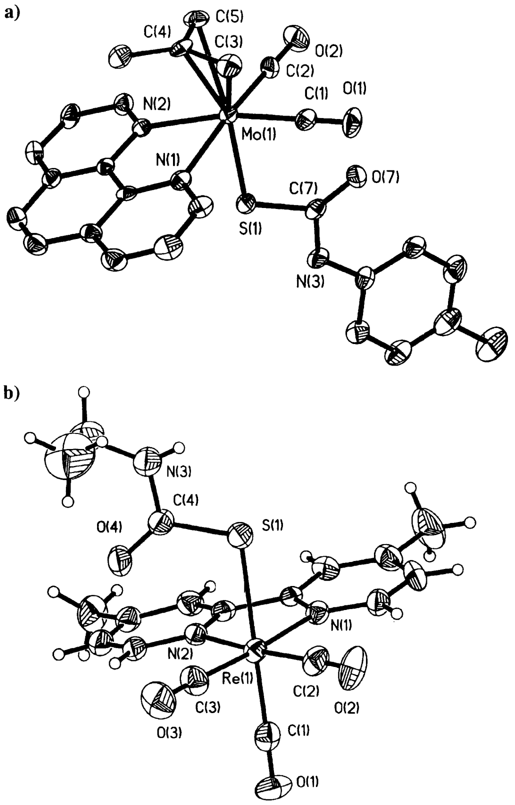

Figure 6. Thermal ellipsoid (30 %) plots showing the molecular structures of the S-bound thiocarbamato complexes **7** (a) and **8b** (b).

In both structures, it can be seen that a molecule of RNCS has been formally inserted into the M–O bond, and that the resultant *N*-alkyl or *N*-aryl thiocarbamate ligand is coordinated through the sulfur atom to the $[Mo(\eta^3\text{-}C_3H_4\text{–}Me\text{-}2)(CO)_2(phen)]$ (**7**) or $[Re(CO)_3(Me_2\text{–}bipy)]$ (**8b**) fragments. For complex **7**, a discussion of bond lengths is precluded because of the low accuracy of the data. The Re–S (2.496(2) Å) distance in **8b** is similar to that found in $[Re[SC(NEt)OMe](CO)_3(bipy)]$ (2.5131(14) Å). The latter complex results from the insertion of RNCS into the Re–O bond of the methoxo complex $[Re(OMe)(CO)_3(bipy)]$.[12] The C(4)–S(1) (1.756(8) Å), C(4)–N(3) (1.339(11) Å) (consistent with single bonds),[39] and C(4)–O(4) (1.210(9) Å) (double bond)[39] distances, as well as the sum of the angles around C(4) (359.9°) support the formulation of the thiocarbamato ligand as depicted in Scheme 7. Moreover, the formation of complexes **7**, **8a**, and **8b** is rationalized in a similar way as for **6** (see above). However, here the putative zwitterionic intermediate would evolve through displacement of oxygen by sulfur (instead of nitrogen), since this softer atom should form the more stable bond to the organometallic fragment. Subsequently, H^+ migration from oxygen to the more basic nitrogen atom would afford the observed products. A stable complex that was isostructural with intermediate A was obtained in the reactions of [Mo(OMe)(η^3-C_3H_4–Me-2)$(CO)_2$(phen)] and [Re(OMe)$(CO)_3$(bipy)] with PhNCS and EtNCS, respectively.[12] In those reactions, the presence of a methyl group in place of hydrogen precluded the final rearrangement.

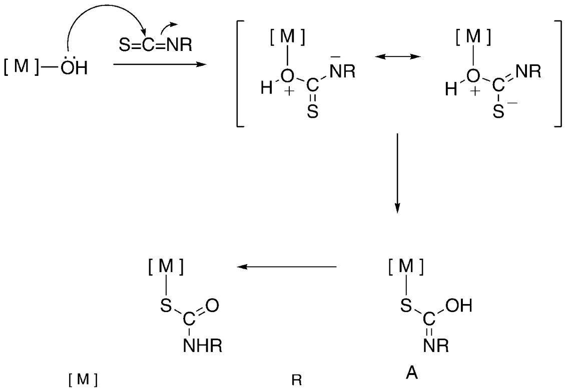

	[M]	R
7	{Mo(η^3-C_3H_4-Me-2)$(CO)_2$(phen)}	*p*-tolyl
8a	{Re$(CO)_3$(Me_2-bipy)}	*p*-tolyl
8b	{Re$(CO)_3$(Me_2-bipy)}	Et

Scheme 7. Proposed mechanism for the formation of **7**, **8a**, and **8b** from hydroxo compounds **1**, **2a**, and **2b**, respectively, upon reaction with isothiocyanates.

Reactions with dimethylacetylenedicarboxylate (DMAD): The complexes [Mo(OH)(η^3-C_3H_4–Me-2)$(CO)_2$(phen)] (**1**) and [Re(OH)$(CO)_3$(N–N)] (**2a**, N–N = bipy; **2b**, N–N = Me_2–bipy) react with DMAD. The reactions take place upon mixing and are accompanied by major changes in the IR spectra. Thus, the two bands for **1** at 1929 and 1843 cm^{-1} were substituted by a single, strong absorption at 1947 cm^{-1} in product **9**. A single IR ν_{CO} band in the carbonyl ligand region is consistent with the existence of either a *trans*-dicarbonyl or a monocarbonyl fragment, both of which are very rare for pseudo-octahedral molybdenum–allyl complexes.[41] Analogously, for the rhenium complexes, the *fac*-Re$(CO)_3$ IR patterns were replaced by two sets of bands of similar intensity and width; this is diagnostic of the *cis*-dicarbonyl moieties in **10a** and **10b**. The ^{1}H NMR spectra of the molybdenum and rhenium products displayed two three-hydrogen singlets, which correspond to two different methoxycarbonyl groups, and the ^{13}C NMR spectra (see Experimental Section) also indicated that these molecules were not symmetrical. The structures of [Mo[C(OH)C(CO_2Me)C(CO_2-Me)O](η^3-C_3H_4–Me-2)$(CO)_2$(phen)] (**9**; Figure 7) and [Re-[C(OH)C(CO_2Me)C(CO_2Me)O]$(CO)_3$(Me_2–bipy)] (**10b**; Figure 8) were determined by X-ray diffraction.[20]

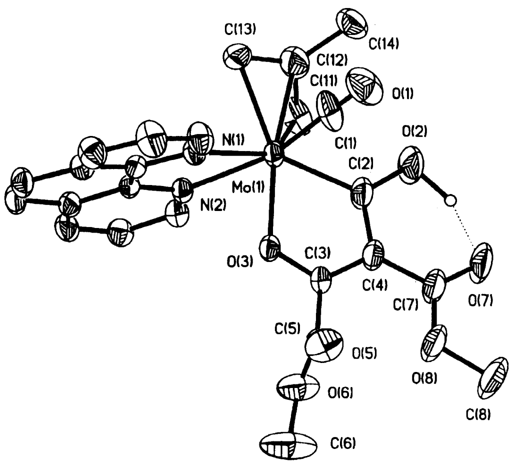

Figure 7. Thermal ellipsoid (30%) plot of **9**.

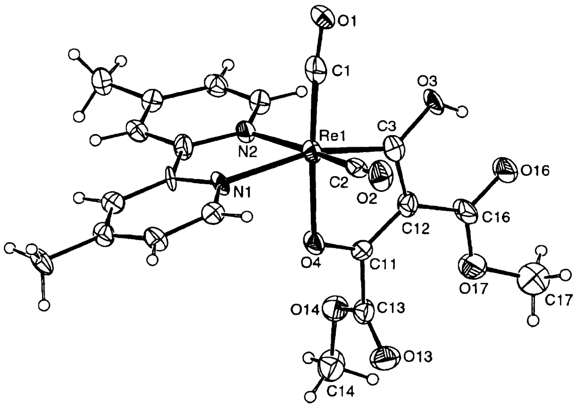

Figure 8. Thermal ellipsoid (30%) plot of **10b**.

The molecules consist of [Mo(η^3-C_3H_4–Me-2)(CO)(phen)] (**9**) and *cis*-[Re$(CO)_2$(Me_2–bipy)] (**10b**) fragments, which are linked to five-membered M–C(OH)–C(CO_2Me)–C(CO_2Me)–O metallacycles that result from the coupling of the hydroxo ligand, DMAD, and one of the CO ligands.

The relatively short Mo–C(2) and Re–C(3) distances (2.054(7) and 2.032(15) Å, respectively), together with the ^{13}C NMR chemical shift for C(2) in **9** ($\delta = 226.95$ ppm) and C(3) in **10b** ($\delta = 278.61$ ppm) indicate that one end of the metallacycle contains a hydroxycarbene group. A compound closely related to **10b** has recently been obtained by us from the reaction of diethylacetylenedicarboxylate with the amido complex [Re(NH*p*Tol)$(CO)_3$(bipy)] (Scheme 8).[33] In view of the crystal structures, it is clear that the NMR spec-

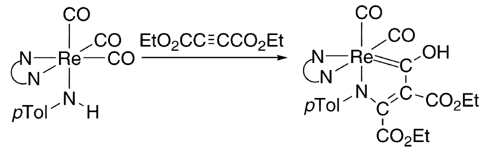

Scheme 8. Reaction of the rhenium amido complex with DMAD afforded a metallacycle.

tra of the products of DMAD insertion can be attributed to solution structures, as well as to those found in the solid state.

A mechanistic rationale that explains the formation of **9**, **10a**, and **10b** is shown in Scheme 9, and is analogous to the one proposed for the reaction with the amido complex. After initial nucleophilic attack of one of the acetylenic carbons of DMAD by the hydroxo (or amido) group, the carbanionic end of the resultant zwitterion attacks a proximal CO ligand. Subsequent H^+ migration from the positively-charged oxygen (or nitrogen) bonded to molybdenum or rhenium to the negatively charged oxygen generates the observed metallacyclic hydroxycarbene.

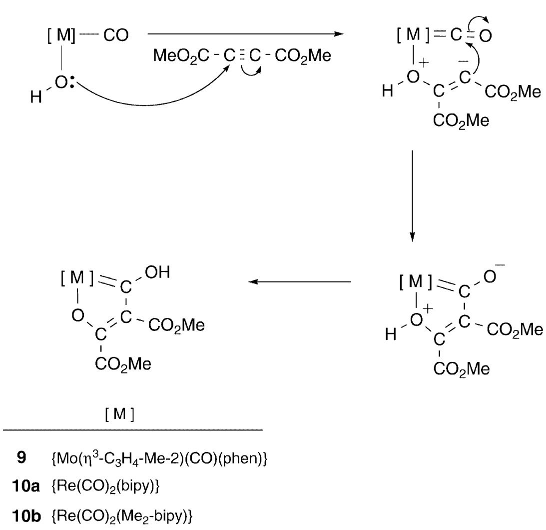

Scheme 9. Reaction of the hydroxo complexes **1**, **2a**, and **2b** with DMAD afforded the new complexes **9**, **10a**, and **10b**, respectively. The metallacycles were the result of coupling between the hydroxo ligand, DMAD, and one of the CO ligands.

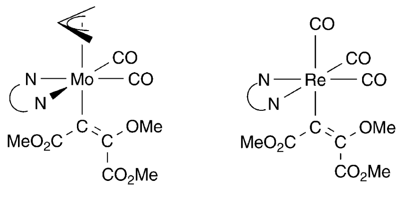

Scheme 10. The *Z*-alkenyl complexes of Mo and Re were obtained by reaction of the methoxo complexes with DMAD.

These results contrast with those obtained for the reaction of DMAD with the methoxo complexes [Mo(OMe)(η^3-C_3H_4–Me-2)$(CO)_2$(phen)] and [Re(OMe)$(CO)_3$(bipy)]. These reactions afford the *Z*-alkenyl complexes shown in Scheme 10 as a result of the displacement of the metal-bonded oxygen by the carbanionic end of a zwitterionic intermediate similar to the one included in Scheme 9.[12] The similar formation of an alkenyl complex as a result of formal DMAD insertion into an Ir–OH bond has also been reported by Bergman.[10] These differences suggest that H^+ migration to the carbonyl oxygen makes an important contribution to the formation of the metallacycles observed by us.[42] Other than this, the only reaction of a hydroxo complex with an acetylene of which we are aware is that of DMAD with the complex [Os(H)(OH)(P*i*Pr_3)(CO)]. This reaction affords the product from formal insertion of DMAD into the O–H bond.[9c] A major difference with the complexes employed in the present study is that the osmium hydroxo complex is pentacoordinate; this allows coordination of Lewis bases, and thus, a mechanism that involves initial coordination of DMAD to Os followed by an intramolecular insertion. With regard to the reactions that afford metallacycles **9**, **10a**, and **10b**, the formation of similar metallacycles with either Mo^{II} or Re^{II} occurs because two carbonyl ligands are adjacent to the OH group in each pseudo-octahedral precursor. Remarkably, [Mo(η^3-allyl)$(CO)_2$(N–N)] and [Re$(CO)_3$(N–N)] fragments in pseudo-octahedral complexes like the ones dealt with in the present study have been found to be rather inert. Thus, the carbonyl ligands have never been found to be the target of nucleophilic attack, even when strong nucleophiles were employed as reagents.[12,14,43]

Conclusion

The reaction of [Re(OTf)$(CO)_3$(N–N)] (**1a** and **1b**) with KOH leads to [Re(OH)$(CO)_3$(N–N)] (**2a** or **2b**) and [{Re$(CO)_3$(bipy)}$_2$(μ-OH)]OTf (**3**-OTf). Which product is formed depends upon the presence or absence of water in the reaction medium.

The reactivity of complexes [Mo(OH)(η^3-C_3H_4–Me-2)$(CO)_2$(phen)] (**1**) and [Re(OH)$(CO)_3$(N–N)] (**2a** and **2b**) toward organic electrophiles is comparable to that of the Group 8–10 metal-hydroxo complexes.[5b,9,10] Unsaturated electrophiles afford the products from formal insertion into the M–O or O–H bonds. The formation of these products is rationalized by means of mechanistic schemes that are similar to those proposed in previous studies of related alkoxo and amido complexes.[12b,40]

Experimental Section

General procedures: All manipulations were carried out under nitrogen using standard Schlenk techniques. Solvents were distilled from Na (hexanes), Na/benzophenone (tetrahydrofuran), or CaH_2 (CH_2Cl_2, CH_3OH,

CH_3CH_2OH). CD_2Cl_2 and CD_3COCD_3 were dried over 4 Å molecular sieves and CD_2Cl_2 was stored in the dark over Na_2CO_3. Elemental analyses were obtained by using a Perkin-Elmer 240-B microanalyzer. The IR spectra were recorded on a Perkin-Elmer FT 1720-X spectrophotometer, while the ^1H, ^{19}F, and $^{13}C\{^1H\}$ NMR spectra were recorded on a Bruker AC-200, AC-300, or DPX-300 spectrometer.

The complexes $[Mo(\eta^3\text{-}C_3H_4\text{–}Me\text{-}2)(OH)(CO)_2(phen)]$[14] and $[Re(OTf)(CO)_3(N\text{–}N)]$[44] were synthesized according to literature procedures.

Crystal structure determination for compounds 4, 5, 7, 8b, and 9: Raw frame data were integrated with the SAINT[45] program. The structures were solved by direct methods with SHELXTL.[46] A semi-empirical absorption correction was applied with the SADABS program.[47] All non-hydrogen atoms were refined anisotropically, while hydrogen atoms were set in calculated positions and refined as riding atoms with a common thermal parameter. All calculations and graphics were made with SHELXTL.

Crystal structure determination for 6 and 10b: Crystal structures were solved by Patterson methods using the Dirdif program.[48] Anisotropic least-squares refinement was carried out with SHELXL-97.[49] All non-hydrogen atoms were anisotropically refined, while hydrogen atoms were geometrically placed and refined as riding on their parent atoms. Empirical absorption corrections were applied by using XABS2.[50] Geometrical calculations were made with PARST,[51] and the crystallographic plots were made with PLATON.[52]

Crystallographic data for compounds **4**, **5**, **6**, **7**, **8b**, **9**, and **10b** are shown in Table 1, Table 2, and Table 3. CCDC-219665 (**3**-BF_4), CCDC-219666 (**4**), CCDC-219667 (**5**), CCDC-219668 (**6**), CCDC-219669 (**7**), CCDC-219670 (**8b**), CCDC-219671 (**9**), and CCDC-219672 (**10b**) contain the supplementary crystallographic data for this paper. These data can be obtained free of charge via www.ccdc.cam.ac.uk/conts/retrieving.html (or from the Cambridge Crystallographic Data Centre, 12, Union Road, Cambridge CB21EZ, UK; fax: (+44)1223-336-033; or deposit@ccdc.cam.ac.uk).

Table 1. Crystal data for **3**-BF_4, **4**, and **5**.

	3-BF_4	**4**	**5**
formula	$C_{26}H_{17}BF_4N_4O_7Re_2$	$C_{17}H_{15}N_2O_5Re$	$C_{52}H_{44}Mo_2N_6O_8{\cdot}2\,CH_2Cl_2$
Fw	956.65	513.51	1242.66
crystal system	triclinic	orthorhombic	triclinic
space group	$P\bar{1}$	*Pbca*	$P\bar{1}$
a [Å]	8.6051(18)	8.4658(11)	12.390(2)
b [Å]	10.694(2)	14.1972(19)	15.144(3)
c [Å]	17.201(4)	28.909(4)	15.957(3)
α [°]	103.892(4)	90	73.848(4)
β [°]	92.836(4)	90	84.432(4)
γ [°]	108.477(4)	90	70.793(4)
V [Å^3]	1443.7(5)	3474.5(8)	2715.7(9)
Z	2	8	2
T [K]	293(2)	299(2)	299(2)
ρ_{calcd} [g cm^{-3}]	2.201	1.963	1.520
$F(000)$	896	1968	1260
$\lambda(Mo_{K\alpha})$ [Å]	0.71073	0.71073	0.71073
crystal size [mm]	0.08 × 0.12 × 0.21	0.06 × 0.10 × 0.27	0.08 × 0.24 × 0.25
μ [mm^{-1}]	8.454	7.024	0.717
scan range [°]	$1.23 \leq \theta \leq 23.30$	$1.41 \leq \theta \leq 23.37$	$1.33 \leq \theta \leq 23.28$
reflections measured	6334	14670	12261
independent reflections	4065	2513	7736
data/restraints/parameters	4065/0/401	2513/0/230	7736/0/672
goodness-of-fit on F^2	1.096	1.069	1.005
R_1/R_{w2} [$I > 2\sigma(I)$]	0.0562/0.1618	0.0270/0.0729	0.0456/0.1206
R_1/R_{w2} (all data)	0.0666/0.1686	0.0410/0.0775	0.0643/0.1311

Table 2. Crystal data for **6**, **7**, and **8b**.

	6	**7**	**8b**
formula	$C_{20}H_{14}N_3O_5Re$	$C_{26}H_{22}MoN_3O_3S{\cdot}CH_2Cl_2$	$C_{18}H_{18}N_3O_4ReS$
Fw	562.54	637.39	558.61
Crystal system	monoclinic	triclinic	orthorhombic
space group	$P2_1/n$	$P\bar{1}$	$P2_12_12_1$
a [Å]	8.7411(3)	12.693(2)	10.101(3)
b [Å]	14.5576(4)	14.370(3)	10.326(3)
c [Å]	15.1477(4)	16.305(3)	19.595(6)
α [°]	90	85.861(4)	90
β [°]	102.471(2)	75.768(3)	90
γ [°]	90	77.325(3)	90
V [Å^3]	1882.06(10)	2812.0(9)	2043.8(10)
Z	4	4	4
T [K]	120(2)	299(2)	293(2
ρ_{calcd} [g cm^{-3}]	1.985	1.506	1.815
$F(000)$	1080	1292	1080
$\lambda(Mo_{K\alpha})$ [Å]	1.54180	0.71073	0.71073
crystal size [mm]	0.28 × 0.13 × 0.08	0.10 × 0.13 × 0.24	0.10 × 0.14 × 0.28
μ [mm^{-1}]	12.974	0.764	6.075
scan range [°]	$4.26 \leq \theta \leq 68.30$	$1.29 \leq \theta \leq 23.31$	$2.08 \leq \theta \leq 23.34$
reflections measured	19225	12840	9224
independent reflections	3446	8002	2958
data/restraints/parameters	3446/1/265	8002/0/665	2958/0/251
goodness-of-fit on F^2	1.251	1.004	1.003
R_1/R_{w2} [$I > 2\sigma(I)$]	0.0485/0.1770	0.0580/0.1214	0.0264/0.0601
R_1/R_{w2} (all data)	0.0523/0.2004	0.1023/0.1347	0.0288/0.0610

Preparation of $[\{Re(CO)_3(bipy)\}_2(\mu\text{-}OH)]OTf$ (3-OTf): KOH (0.240 g, 0.435 mmol) was added to a solution of $[Re(OTf)(CO)_3(bipy)]$ (0.200 g, 0.347 mmol) in CH_2Cl_2 (20 mL), and the mixture was allowed to stir for 12 h at room temperature. The yellow solution was filtered by cannula and concentrated under vacuum to a volume of 5 mL. The residue was layered with hexane (20 mL) and cooled to −20 °C to afford yellow crystals of **3**-OTf; yield: 0.031 g, 71 %; ^1H NMR (CD_2Cl_2, 25 °C): $\delta = 8.91$ (m, 4H; bipy), 8.22 (m, 8H; bipy), 7.58 (m, 4H; bipy), −1.64 ppm (br s, 1H; OH); IR (CH_2Cl_2): $\tilde{\nu} = 2018$ vs, 1910 s, 1889 s cm^{-1} (CO); IR (KBr): $\tilde{\nu} = 3645$ br cm^{-1} (OH); elemental analysis calcd (%) for $C_{27}H_{17}F_3N_4O_{10}Re_2S$: C 31.82, H 1.68, N 5.49; found: C 31.86, H 1.62, N 5.14.

Independent preparation of $[\{Re(CO)_3(bipy)\}_2(\mu\text{-}OH)]BF_4$ (3-BF_4): $HBF_4{\cdot}OEt_2$ (11 μL, 0.075 mmol) was added to a solution of **2a** (0.070 g, 0.151 mmol) in CH_2Cl_2 (15 mL) at −78 °C, and the mixture was allowed to reach room temperature. The color of the solution changed from orange to yellow. The solution was concentrated under vacuum to a volume of 5 mL, and the residue was layered with hexane (20 mL) and cooled to −20 °C to afford yellow crystals of **3**-BF_4. One crystal was used for structure determination by X-ray diffraction; yield: 0.060 g, 84 %; ^1H NMR (CD_2Cl_2, 25 °C): $\delta = 8.91$ (m, 4H; bipy), 8.22 (m, 8H; bipy), 7.58 (m, 4H; bipy), −1.64 ppm (br s, 1H; OH); ^{13}C NMR (CD_2Cl_2, 25 °C): $\delta = 199.33$ (2CO), 193.09 (CO), 157.68, 155.73, 142.28, 130.12, 126.17 ppm (bipy); IR (CH_2Cl_2): $\tilde{\nu} = 2018$ vs, 1910 s, 1889 s cm^{-1} (CO); IR (KBr): $\tilde{\nu} = 3645$ br cm^{-1} (OH); elemental analysis calcd (%) for

Table 3. Crystal data for **9** and **10b**.

	9	**10b**
formula	$C_{24}H_{22}MoN_2O_7{\cdot}0.5\,CH_2Cl_2$	$C_{21}H_{18}N_2O_8Re{\cdot}1.5\,CH_2Cl_2$
Fw	582.43	739.96
crystal system	monoclinic	monoclinic
space group	$C2/c$	$P2_1/c$
a [Å]	26.064(4)	11.5690(6)
b [Å]	16.990(3)	11.0920(6)
c [Å]	13.420(2)	20.8256(6)
α [°]	90	90
β [°]	120.787(3)	94.307(3)
γ [°]	90	90
V [Å^3]	5105.2(15)	2664.9(2)
Z	8	4
T [K]	2938(2)	120(2)
ρ_{calcd} [g cm^{-3}]	1.516	1.844
F(000)	2348	1440
$\lambda(Mo_{K\alpha})$ [Å]	0.71073	1.54180
crystal size [mm]	0.12 × 0.21 × 0.33	0.25 × 0.12 × 0.02
μ [mm^{-1}]	0.564	12.118
scan range [°]	$1.82 \leq \theta \leq 23.26$	$3.83 \leq \theta \leq 68.70$
reflections measured	11199	37972
independent reflections	3669	4865
data/restraints/parameters	3669/0/347	4865/17/336
goodness-of-fit on F^2	1.041	0.872
R_1/R_{w2} [$I > 2\sigma(I)$]	0.0512/0.1319	0.0586/0.1404
R_1/R_{w2} (all data)	0.0686/0.1495	0.1035/0.1646

$C_{26}H_{17}BF_4N_4O_7Re_2$: C 32.64, H 1.79, N 5.85; found: C 32.58, H 1.71, N 5.90.

Reaction of 2b with phenyl acetate: A 5 mm NMR tube was charged with a solution of **2b** (0.020 g, 0.042 mmol) in CD_2Cl_2 (0.5 mL) and was then capped with a rubber septum. PhOAc (6.5 μL, 0.042 mmol) was injected, and the reaction was monitored by ^{1}H NMR spectroscopy. After 20 h at room temperature, the color of the solution changed from orange to yellow and the ^{1}H NMR spectrum showed signals for phenol [$\delta = 7.25$ (m, 2H; Ph), 6.90 (m, 1H; Ph), 6.45 (m, 2H; Ph), 5.25 ppm (brs, 1H; OH)] and complex [Re(OAc)(CO)$_3$(Me$_2$–bipy)] (**4**) (see below).

This reaction was also carried out on a preparative scale, in which 0.080 g of **2b** (0.169 mmol) and a stoichiometric amount of PhOAc (22 μL, 0.169 mmol) was employed. Slow diffusion of hexane into a concentrated solution of **4** in CH_2Cl_2 afforded yellow crystals, one of which was suitable for an X-ray experiment; yield: 0.093 g, 94%; ^{1}H NMR (CD_2Cl_2, 25 °C): $\delta = 8.95$ (d, $J = 5.6$ Hz, 2H; Me$_2$–bipy), 8.03 (s, 2H; Me$_2$–bipy), 7.37 (d, $J = 5.6$ Hz, 2H; Me$_2$–bipy), 2.59 (s, 6H; Me$_2$–bipy), 1.54 ppm (s, 3H; CH_3CO_2); ^{13}C NMR (CD_2Cl_2, 25 °C): $\delta = 199.37$ (2CO), 195.36 (CO), 176.55 (CH_3CO_2), 155.78, 153.51, 152.16, 127.89, 123.87 (Me$_2$–bipy), 23.36 (CH_3CO_2), 21.84 ppm (Me$_2$–bipy); IR (CH_2Cl_2): $\tilde{\nu} = 2017$ vs, 1913 s, 1887 s (CO), 1620 cm^{-1} (C=O); elemental analysis calcd (%) for $C_{17}H_{15}N_2O_5Re$: C 39.76, H 2.94, N 5.45; found: C 39.74, H 2.99, N 5.60.

Reaction of 1 with phenyl acetate: PhOAc (5 μL, 0.039 mmol) was added to a solution of **1** (0.016 g, 0.039 mmol) in CH_2Cl_2 (10 mL), and the reaction was monitored by IR spectroscopy. After 8 h, the IR spectrum showed the disappearance of the bands for **1** (IR $\tilde{\nu} = 1934$ and 1844 cm^{-1}), while two new bands were assigned to the acetate complex [Mo(OAc)(η^3-C_3H_4–Me-2)(CO)$_2$(phen)]. The solution was concentrated in vacuo and upon addition of hexane, a red-brown solid precipitated. This was washed with hexane and dried under vacuum; yield: 0.016 g, 92%; ^{1}H NMR (CD_2Cl_2, 25 °C): $\delta = 9.17$ (d, $J = 3.9$ Hz, 2H; H$_{2,9}$), 8.50 (d, $J = 7.3$ Hz, 2H; H$_{4,7}$), 7.90 (s, 2H; H$_{5,6}$), 7.71 (m, 2H; H$_{3,8}$), 2.98 (s, 2H; H$_s$), 1.46 (s, 2H; H$_a$), 1.31 (s, 3H; CH_3CO_2), 0.78 ppm (s, 3H; η^3-C_3H_4(CH_3)-2); IR (CH_2Cl_2): $\tilde{\nu} = 1948$ vs, 1874 s cm^{-1}; elemental analysis calcd (%) for $C_{20}H_{18}MoN_2O_4$: C 53.82, H 3.92, N 6.27; found: C 53.58, H 4.30, N 6.47.

Reaction of 2b with vinyl acetate: Complex **2b** (0.020 g, 0.042 mmol) was dissolved in CD_2Cl_2 (0.5 mL) in a 5 mm NMR tube capped with a rubber septum. Vinyl acetate (4 μL, 0.043 mmol) was injected and the reaction was monitored by ^{1}H NMR spectroscopy. After 12 h at room temperature, the color of the solution changed from orange to yellow and the ^{1}H NMR spectrum showed signals for acetaldehyde [9.76 (s, 1H; CH_3CHO), 2.16 ppm (s, 3H; CH_3CHO)] and complex **4**.

Reaction of 1 with (*p*-tolyl)NCO: (*p*-tolyl)NCO (22 μL, 0.170 mmol) was added to a solution of **1** (0.070 g, 0.168 mmol) in THF (10 mL). The mixture was stirred for 15 min and was then evaporated to dryness. The residue was dissolved in CH_2Cl_2, filtered through diatomaceous earth, and concentrated in vacuo to 5 mL. Upon addition of hexane (20 mL), a red microcrystalline solid precipitated. This was washed with hexane (3 × 10 mL) and dried under vacuum. The solid was dissolved in CH_2Cl_2 (5 mL) and layered with diethyl ether (20 mL). After three days at room temperature, red crystals of **5**·*N,N'*-di(*p*-tolyl)urea were obtained, one of which was used for X-ray analysis; yield: 0.075 g, 71%; ^{1}H NMR (CD_2Cl_2, 25 °C): $\delta = 9.18$ (dd, $J = 5.0$ and 1.3 Hz, 4H; H$_{2,9}$), 8.52 (dd, $J = 8.3$ Hz, 4H; H$_{4,7}$), 7.99 (s, 4H; H$_{5,6}$), 7.85 (dd, 4H; H$_{3,8}$), 7.06, 7.03, 6.95, 6.57 (AB quartet, 8H; *p*-tol), 2.98 (s, 4H; H$_s$), 2.38 (s, 6H; C_6H_4–CH_3), 1.46 (s, 4H; H$_a$), 0.78 ppm (s, 6H; η^3-C_3H_4(CH_3)-2); IR (THF): $\tilde{\nu} = 1953$ vs, 1874 s, 1516 m cm^{-1}; elemental analysis calcd (%) for $C_{52}H_{44}Mo_2N_6O_8{\cdot}2\,CH_2Cl_2$: C 52.10, H 4.04, N 6.75; found: C 52.39, H 4.26, N 7.12.

Reaction of 2a with PhNCO: PhNCO (11 μL, 0.104 mmol) was added to a solution of **2a** (0.050 g, 0.104 mmol) in THF (20 mL), and the color of the solution changed instantly from orange to yellow. The solvent was removed under vacuum and the yellow solid was dissolved in CH_2Cl_2 (5 mL). Slow diffusion of diethyl ether into this solution at room temperature afforded orange crystals of **6**, one of which was employed for an X-ray structure determination; yield: 0.052 g, 90%; ^{1}H NMR (CD_2Cl_2, 25 °C): $\delta = 9.11$ (m, 2H; bipy), 8.12 (m, 4H; bipy), 7.57 (m, 2H; bipy), 6.96 (m, 5H; Ph), 6.69 ppm (brs, 1H; NH); IR (CH_2Cl_2): $\tilde{\nu} = 2019$ vs, 1917 s, 1889 s cm^{-1} (CO); elemental analysis calcd (%) for $C_{20}H_{14}N_3O_5Re$: C 42.70, H 2.50, N 7.46; found: C 42.76, H 2.61, N 7.40.

Reaction of 1 with (*p*-tolyl)NCS: (*p*-tolyl)NCS (19 μL, 0.150 mmol) was added to a solution of **1** (0.060 g, 0.150 mmol) in THF (15 mL), and the mixture was stirred for 1 h. The red solution was concentrated in vacuo, layered with hexane (15 mL), and stored at −20 °C to afford red crystals of **7**, one of which was used for X-ray analysis; yield: 0.070 g, 73%; ^{1}H NMR (CD_2Cl_2, 25 °C): $\delta = 9.05$ (d, $J = 3.9$ Hz, 2H; H$_{2,9}$), 8.47 (d, $J = 7.3$ Hz, 2H; H$_{4,7}$), 7.95 (s, 2H; H$_{5,6}$), 7.83 (m, 2H; H$_{3,8}$), 7.43 (brs, 1H; NH), 7.22, 7.18, 7.01, 6.97 (AB quartet, 4H; *p*-tol), 2.98 (s, 2H; H$_s$), 2.23 (s, 3H; C_6H_4–CH_3), 1.64 (s, 2H; H$_a$), 0.61 ppm (s, 3H; η^3-C_3H_4(CH_3)-2); IR (THF): $\tilde{\nu} = 1956$ vs, 1885 s cm^{-1} (CO); elemental analysis calcd (%) for $C_{26}H_{22}MoN_3O_3S{\cdot}CH_2Cl_2$: C 50.79, H 3.94, N 6.58; found: C 50.66, H 4.01, N 6.66.

Reaction of 2b with (*p*-tolyl)NCS: (*p*-tolyl)NCS (8 μL, 0.054 mmol) was added to a solution of **2b** (0.025 g, 0.053 mmol) in THF (10 mL). The resultant yellow solution was stirred for 15 min, the solvent was then removed in vacuo, and the residue was dissolved in CH_2Cl_2 (3 mL). Upon addition of hexane (10 mL), a yellow microcrystalline solid precipitated. This was washed with hexane and dried under vacuum; yield: 0.020 g, 61%; ^{1}H NMR (CD_2Cl_2, 25 °C): $\delta = 8.91$ (d, $J = 5.8$ Hz, 2H; Me$_2$–bipy), 7.99 (s, 2H; Me$_2$–bipy), 7.30 (d, $J = 5.8$ Hz, 2H; Me$_2$–bipy), 5.90 (brs, 1H; NH), 2.55 (s, 6H; CH_3 and Me$_2$–bipy), 2.23 ppm (s, 3H; C_6H_4–CH_3); IR (THF): $\tilde{\nu} = 2017$ vs, 1916 s, 1892 s cm^{-1} (CO); elemental analysis calcd (%) for $C_{23}H_{20}N_3O_4ReS$: C 44.50, H 3.24, N 6.77;. found: C 44.39, H 3.13, N 6.95.

Reaction of 2b with EtNCS: EtNCS (15 μL, 0.170 mmol) was added to a solution of **2b** (0.080 g, 0.169 mmol) in THF (20 mL), and the color of the solution changed instantly from orange to yellow. The solvent was removed under vacuum and the yellow solid was dissolved in CH_2Cl_2 (5 mL). Slow diffusion of hexane into this solution at room temperature afforded orange crystals of **8b**, one of which was employed for an X-ray structure determination; yield: 0.077 g, 85%; ^{1}H NMR (CD_2Cl_2, 25 °C): $\delta = 8.89$ (d, $J = 5.5$ Hz, 2H; Me$_2$–bipy), 7.99 (s, 2H; Me$_2$–bipy), 7.30 (d, $J = 5.5$ Hz, 2H; Me$_2$–bipy), 2.99 (q, $J = 6.9$ Hz, 2H; NCH_2CH_3), 2.54 (s, 6H; CH_3 and Me$_2$–bipy), 0.92 ppm (t, $J = 6.9$ Hz, 3H; NCH_2CH_3);

^{1}H NMR (CD_2Cl_2, −40 °C): $\delta = 8.85$ (d, $J = 5.0$ Hz, 2H; Me_2–bipy), 8.00 (s, 2H; Me_2–bipy), 7.30 (d, $J = 5.0$ Hz, 2H; Me_2–bipy), 5.50 (s, 1H; NH), 3.02 (q, $J = 6.9$ Hz, 2H; $NC\mathit{H}_2CH_3$), 2.49 (s, 6H; CH_3 and Me_2–bipy), 0.91 ppm (t, $J = 6.9$ Hz, 3H; $NCH_2C\mathit{H}_3$); ^{13}C NMR (CD_2Cl_2, 25 °C): $\delta =$ 199.87 (2CO), 192.70 (CO), 175.35 (NC(O)S), 157.06, 154.85, 152.81, 129.11, 125.41 (Me_2–bipy), 37.83 ($N\mathit{C}H_2CH_3$), 23.12 (Me_2–bipy), 16.55 ppm ($NCH_2\mathit{C}H_3$); IR (CH_2Cl_2): $\tilde{\nu} = 2016$ vs, 1919 s, 1893 s cm^{-1} (CO); elemental analysis calcd (%) for $C_{18}H_{18}N_3O_4ReS$: C 38.70, H 3.24, N 7.52; found: C 38.67, H 3.31, N 7.50.

Reaction of 1 with dimethylacetylenedicarboxylate: $MeO_2CC{\equiv}CCO_2Me$ (12 μL, 0.098 mmol) was added to a red solution of **1** (0.040 g, 0.092 mmol) in THF (10 mL). The darkened solution was stirred for 15 min, filtered through diatomaceous earth, and concentrated under vacuum. Addition of hexane (10 mL) caused the precipitation of a red-brown microcrystalline solid **9**, which was washed with diethyl ether (2 × 10 mL) and dried under vacuum. Red-brown crystals were obtained by slow diffusion of hexane into a concentrated solution of **9** in THF. One crystal was used for X-ray analysis; yield: 0.028 g, 51 %; ^{1}H NMR (CD_2Cl_2, 25 °C): $\delta = 12.46$ (s, 1H; OH), 9.58 (d, $J = 4.95$ Hz, 1H; phen), 9.13 (brs, 1H; phen), 8.74 (brs, 1H; phen), 8.41 (m, 2H; phen), 7.88 (m, 2H; phen), 7.59 (brs, 1H; phen), 3.69 (s, 3H; OCH_3), 3.66 (s, 1H; H_s), 3.55 (s, 3H; OCH_3), 2.93 (s, 1H; H_s), 2.25 (s, 3H; η^3-$C_3H_4(C\mathit{H}_3)$-2), 1.28 (s, 1H; H_a), 0.55 ppm (s, 1H; H_a); ^{13}C{^{1}H} NMR (CD_2Cl_2, 25 °C): $\delta =$ 226.95 (Mo=C), 206.24 (CO), 167.26 [Mo–O*C*(CO_2Me)], 153.22 (phen), 152.73 (phen), 151.87 (phen), 151.46 (C=O), 146.54 (C=O), 142.53 [C(OH)*C*(CO_2Me)], 139.61 (phen), 138.14 (phen), 138.00 (phen), 137.07 (phen), 130.42 (phen), 130.17 (phen), 127.63 (phen), 127.45 (phen), 124.74 (phen), 82.92 (C_2 allyl), 55.45 (OCH_3), 55.18 (OCH_3), 20.41 ppm (η^3-$C_3H_4(\mathit{C}H_3)$-2); IR (THF): $\tilde{\nu} = 1947$ cm^{-1}; elemental analysis calcd (%) for $C_{24}H_{22}MoN_2O_7 \cdot 0.5\,CH_2Cl_2$: C 49.97, H 3.93, N 4.75; found: C 50.22, H 3.89, N 4.97.

Reaction of 2a with dimethylacetylenedicarboxylate: $MeO_2CC{\equiv}CCO_2Me$ (10 μL, 0.083 mmol) was added to a solution of **2a** (0.040 g, 0.083 mmol) in THF (10 mL), and the color of the solution changed instantly from orange to red. The volatiles were removed under vacuum and the residue solid was dissolved in CH_2Cl_2 (10 mL). Slow diffusion of hexanes into this solution at room temperature afforded red crystals of **10a**; yield: 0.041 g, 84 %; ^{1}H NMR (CD_2Cl_2, 25 °C): $\delta = 13.73$ (brs, 1H; OH), 9.20 (m, 1H; bipy), 8.41 (m, 1H; bipy), 8.00 (m, 2H; bipy), 7.51 (m, 3H; bipy), 7.39 (m, 1H; bipy), 3.70 (s, 3H; OCH_3), 3.66 ppm (s, 3H; OCH_3); ^{13}C{^{1}H} NMR (CD_2Cl_2, 25 °C): $\delta = 268.95$ (Re=C), 205.07 (CO), 199.78 (CO), 168.30 (C=O), 168.09 [Re–O*C*(CO_2Me)], 166.41 (C=O), 156.79, 154.54, 153.66, 152.83 (bipy), 140.65 [C(OH)*C*(CO_2Me)], 139.01, 137.76 (bipy), 127.29, 127.24, 123.28, 122.91 (bipy), 52.50 (OCH_3), 51.61 ppm (OCH_3); IR (CH_2Cl_2): $\tilde{\nu} = 1929$ vs, 1853 s cm^{-1}; elemental analysis calcd (%) for $C_{19}H_{17}N_2O_8Re$: C 38.84, H 2.94, N 4.76; found: C 38.89, H 2.99, N 4.68.

Reaction of 2b with dimethylacetylenedicarboxylate: Following the procedure described above for **10a**, **10b** was prepared by reaction of **2b** (0.080 g, 0.169 mmol) and $MeO_2CC{\equiv}CCO_2Me$ (21 μL, 0.170 mmol) in THF (10 mL). Slow diffusion of hexanes into a solution of **10b** in CH_2Cl_2 at room temperature afforded red crystals, one of which was used for the structure determination of **10b** by X-ray diffraction; yield: 0.086 g, 67 %; ^{1}H NMR (CD_2Cl_2, 25 °C): $\delta = 13.67$ (brs, 1H; OH), 9.01 (d, $J = 5.5$ Hz, 1H; Me_2–bipy), 8.23 (d, $J = 5.5$ Hz, 1H; Me_2–bipy), 7.98 (m, 2H; Me_2–bipy), 7.31 (d, $J = 5.5$ Hz, 1H, Me_2–bipy), 7.22 (d, $J = 5.5$ Hz, 1H; Me_2–bipy), 3.70 (s, 3H; OCH_3), 3.67 (s, 3H; OCH_3), 2.54 (s, 3H; CH_3 and Me_2–bipy), 2.51 ppm (s, 3H; CH_3 and Me_2–bipy); ^{13}C{^{1}H} NMR (CD_2Cl_2, 25 °C): $\delta = 278.61$ (Re=C), 207.31 (CO), 201.29 (CO), 169.71 (C=O), 167.89 [Re–O*C*(CO_2Me)], 165.71 (C=O), 157.95, 156.04, 155.88, 153.59, 152.88, 151.54 (Me_2–bipy), 135.21 [C(OH)*C*(CO_2Me)], 129.44, 125.26, 124.93 (Me_2–bipy), 53.84 (OCH_3), 52.93 (OCH_3), 23.15 (CH_3 and Me_2–bipy), 23.02 ppm (CH_3 and Me_2–bipy); IR (CH_2Cl_2): $\tilde{\nu} = 1925$, 1840 cm^{-1}; elemental analysis calcd (%) for $C_{21}H_{18}N_2O_8Re \cdot 1.5\,CH_2Cl_2$: C 36.20, H 2.90, N 3.82; found: C 36.11, H 3.09, N 5.65.

Acknowledgements

We thank Ministerio de Ciencia y Tecnología, Ministerio de Educación, Ministerio de Asuntos Exteriores, and Principado de Asturias for support of this work (grants BQU2003-08649, BQU2000-0219, BQU-2002-03414, PR-01-GE-4, and PR-01-GE-7), as well as for a predoctoral fellowship (to E.H.) and travel grants (to D.C.G. and M.E.N.C.).

---

[1] Alkoxo complexes: a) M. H. Chisholm, *J. Chem. Soc. Dalton Trans.* **1996**, 1781–1791; b) M. H. Chisholm, *Chem. Soc. Rev.* **1995**, *24*, 79–88; c) W. E. Buhro, M. H. Chisholm, *Adv. Organomet. Chem.* **1987**, *27*, 311–369; d) R. R. Schrock, *Polyhedron* **1995**, *14*, 3177–3195; e) C. C. Cummins, *Chem. Commun.* **1998**, 1777–1785; amido complexes: f) R. Kempe, *Angew. Chem.* **2000**, *112*, 478; *Angew. Chem. Int. Ed.* **2000**, *39*, 468–493. For a general (not limited to coordination compounds) monography on alkoxo and aryloxo compounds see: g) D. C. Bradley, R. C. Mehrotra, I. P. Rothwell, A. Singh, *Alkoxo and Aryloxo Derivatives of Metals*, Academic Press, **2001**, London. Reviews dealing with hydroxo, alkoxo, and amido complexes of low valent late transition metals: h) H. E. Bryndza, W. Tam, *Chem. Rev.* **1988**, *88*, 1163–1188; i) R. G. Bergman, *Polyhedron* **1995**, *14*, 3227–3237.

[2] F. Basolo, R. G. Pearson, *Mechanisms of Inorganic Reactions*, 2nd ed, Wiley, New York, **1968**, pp. 177. For a recent study where this effect is found to be important in transformations of organometallic compounds see: T. C. Flood, J. K. Lim, M. A. Deming, W. Keung, *Organometallics* **2000**, *19*, 1166–1174.

[3] H. E. Bryndza, L. K. Fong, R. A. Paciello, W. Tam, J. E. Bercaw, *J. Am. Chem. Soc.* **1987**, *109*, 1444–1456.

[4] a) J. M. Mayer, *Comments Inorg. Chem.* **1988**, *8*, 125–135; b) K. G. Caulton, *New J. Chem.* **1994**, *18*, 25–41. For an alternative interpretation see: c) P. L. Holland, R. A. Andersen, R. G. Bergman, *Comments Inorg. Chem.* **1999**, *21*, 115–129.

[5] a) F. Bottomley, L. Sutin, *Adv. Organomet. Chem.* **1988**, *28*, 339–396; b) M. A. Bennett, H. Jin, S. Li, L. M. Rendina, A. C. Willis, *J. Am. Chem. Soc.* **1995**, *117*, 8335–8340; c) A. Maldotti, C. Bartocci, G. Varani, A. Molinari, P. Battioni, D. Mansuy, *Inorg. Chem.* **1996**, *35*, 1126–1131; d) Y. Yamamoto, X.-H. Han, J.-F. Ma, *Angew. Chem.* **2000**, *112*, 2041; *Angew. Chem. Int. Ed.* **2000**, *39*, 1965–1968; e) A. Mori, Y. Danda, T. Fujii, K. Hirabayashi, K. Osakada, *J. Am. Chem. Soc.* **2001**, *123*, 10774–10775; f) K. L. Breno, D. R. Tyler, *Organometallics* **2001**, *20*, 3864–3868; g) K. L. Breno, M. D. Pluth, D. R. Tyler, *Organometallics* **2003**, *22*, 1203–1211.

[6] J. R. Fulton, A. W. Holland, D. J. Fox, R. G. Bergman, *Acc. Chem. Res.* **2002**, *35*, 44–56.

[7] J. W. Gilje, H. W. Roesky, *Chem. Rev.* **1994**, *94*, 895–910.

[8] S. A. MacGregor, D. MacQueen, *Inorg. Chem.* **1999**, *38*, 4868–4876.

[9] a) R. A. Michelin, M. Napoli, R. Ros, *J. Organomet. Chem.* **1979**, *175*, 239–255; b) J-G. Ren, H. Tomita, M. Minato, T. Ito, K. Osakada, M. Yamasaki, *Organometallics* **1996**, *15*, 852–859; c) A. J. Edwards, S. Elipe, M. A. Esteruelas, F. J. Lahoz, L. A. Oro, C. Valero, *Organometallics* **1997**, *16*, 3828–3836; d) J. Ruiz, M. T. Martínez, F. Florenciano, V. Rodríguez, G. López, J. Pérez, P. A. Chaloner, P. B. Hitchcock, *Inorg. Chem.* **2003**, *42*, 3650–3661; e) C. Bergquist, T. Fillebeen, M. M. Morlok, G. Parkin, *J. Am. Chem. Soc.* **2003**, *125*, 6189–6199.

[10] K. A. Woerpel, R. G. Bergman, *J. Am. Chem. Soc.* **1993**, *115*, 7888–7889.

[11] a) M. D. Fryzuk, C. D. Montgomery, *Coord. Chem. Rev.* **1989**, *95*, 1–40; b) L. M. Green, D. W. Meek, *Organometallics* **1989**, *8*, 659–666; c) A. W. Kaplan, R. G. Bergman, *Organometallics* **1998**, *17*, 5072–5085; d) J. Kovács, T. D. Todd, J. H. Reibenspies, F. Joó, D. J. Darensbourg, *Organometallics* **2000**, *19*, 3963–3969.

[12] a) E. Hevia, J. Pérez, L. Riera, V. Riera, D. Miguel, *Organometallics* **2002**, *21*, 1750–1752; b) E. Hevia, J. Pérez, L. Riera, V. Riera, I. del Río, S. García-Granda, D. Miguel, *Chem. Eur. J.* **2002**, *8*, 4510–4521.

[13] A preliminary communication that includes the reactivity of the rhenium hydroxo complexes toward CS_2 has been published: D. C. Ger-

bino, E. Hevia, D. Morales, M. E. N. Clemente, J. Pérez, L. Riera, V. Riera, D. Miguel, *Chem. Commun.* **2003**, 328–329. Those results are substantially different than the ones included here, and will not be republished in the present paper.

[14] D. Morales, M. E. N. Clemente, J. Pérez, L. Riera, V. Riera, D. Miguel, *Organometallics* **2002**, *21*, 4934–4938.

[15] The hydroxo complexes **2a** and **2b** were previously synthesized by a similar method, see ref. [16]. We mentioned their preparation here to show that the presence or absence of water has the same effect as for the aforementioned molybdenum complexes. Experimental details are given as Supporting Information.

[16] a) D. H. Gibson, X. Yin, *J. Am. Chem. Soc.* **1998**, *120*, 11200–11201; b) D. H. Gibson, X. Yin, H. Hen, M. S. Mashuta, *Organometallics* **2003**, *22*, 337–346.

[17] The synthesis of this complex by a different route as its SbF$_6$ salt, and its X-ray characterization were reported when this manuscript was in preparation: P. J. Heard, P. Sroisuwan, D. A. Tocher, *Polyhedron* **2003**, *22*, 1321–1327.

[18] The formation of the bimetallic compound **3**-OTf in the reaction of **1a** with KOH in anhydrous CH$_2$Cl$_2$ can be accounted for if we consider that [Re(OH)(CO)$_3$(bipy)] (**2a**), which would be the primary product of the reaction, is much more soluble in CH$_2$Cl$_2$ than KOH. Thus, nucleophilic displacement of the triflato ligand of **1a** by the non-dissociated hydroxo group of **2a** would lead to the formation of **3**-OTf. As the concentration of **2a** increases, this pathway competes with the reaction of **1a** with the free hydroxide ion, whose concentration in the CH$_2$Cl$_2$ solution is low. On the other hand, in the presence of a large excess of water, the displacement of the triflato ligand of **1a** or **1b** would be affected by water instead of by the hydroxide ion. The product of this step would be [Re(OH$_2$)(CO)$_3$(N–N)]$^+$, whose ligated water molecule would be rendered highly acidic by coordination to the strong Lewis acidic center. Subsequent deprotonation by the basic aqueous solution would lead to the observed products **2a** and **2b**. A similar result, namely formation of either a monometallic hydroxo compound or a hydroxo-bridged bimetallic cation, was found by us in a recent exploration of the reactivity of [MoCl(η^3-methallyl)(CO)$_2$(phenanthroline)] toward KOH, see reference [14].

[19] In this reaction, half of the hydroxo complex is transformed into the cationic aquo complex, whose labile water ligand is then displaced by the hydroxo ligand of the non-reacted hydroxo complex to afford the OH-bridged product.

[20] Tables of distances and angles of all the compounds whose structures were determined by X-ray diffraction are included as Supporting Information.

[21] For complexes of this kind that contain [Mo(η^3-allyl(CO)$_2$] or [Re(CO)$_3$] fragments see reference [22] and reference [23], respectively.

[22] a) K. R. Breakell, S. J. Rettig, A. Storr, J. Trotter, *Can. J. Chem.* **1979**, *57*, 139–146; b) S.-F. Lush, S.-H. Wang, G.-H. Lee, S.-M. Peng, S.-L. Wang, R.-S. Liu, *Organometallics* **1990**, *9*, 1862–1871; c) C. Borgmann, C. Limberg, E. Kaifer, H. Pritzkow, L. Zsolnai, *J. Organomet. Chem.* **1999**, *580*, 214–224; d) C. Borgmann, C. Limberg, S. Cunskis, P. Kircher, *Eur. J. Inorg. Chem.* **2001**, 349–352.

[23] W. Wang, Y. K. Yan, T. S. A. Hor, J. J. Vittal, J. R. Wheaton, I. H. Hall, *Polyhedron* **2002**, *21*, 1991–1999.

[24] a) C. Balzarek, T. J. R. Weakley, L. Y. Kuo, D. R. Tyler, *Organometallics* **2000**, *19*, 2927–2931; b) R. W. McGaff, N. C. Dopke, R. K. Hayashi, D. R. Powell, P. M. Treichel, *Polyhedron* **2000**, *19*, 1245–1254.

[25] E. Hevia, J. Pérez, V. Riera, D. Miguel, S. Kassel, A. Rheingold, *Inorg. Chem.* **2002**, *41*, 4673–4679.

[26] W. R. Scheidt, B. Cheng, M. K. Safo, F. Cukiernik, J-C. Marchon, P. G. Debrunner, *J. Am. Chem. Soc.* **1992**, *114*, 4420–4421.

[27] For reactions of organometallic complexes with isocyanates see: P. Braunstein, D. Nobel, *Chem. Rev.* **1989**, *89*, 1927–1945.

[28] K. Nakamoto, *Infrared and Raman Spectra of Inorganic and Coordination compounds. Part B: Applications in Coordination, Organometallic and Bioinorganic Chemistry*, 5th ed. Wiley, **1997**, New York.

[29] A. G. Orpen, L. Brammer, F. H. Allen, O. Kennard, D. G. Watson, R. Taylor, *J. Chem. Soc. Dalton Trans.* **1989**, *1*-83.

[30] η^1(O)-η^1(O): a) Ref. [9d] and [16b]; b) R. A. Michelin, G. Strukul, N. Bresciani-Pahor, E. Zangrando, L. Randaccio, *Inorg. Chim. Acta* **1984**, *84*, 229–232; c) M. K. Reinking, J. Ni, P. E. Fanwick, C. P. Kubiak, *J. Am. Chem. Soc.* **1989**, *111*, 6459–6461; d) D. A. Brown, D. M. Kimari, A. M. Duzs-Moore, T. A. Budzichowski, D. M. Ho, S. K. Mandal, *J. Organomet. Chem.* **2002**, *658*, 88–93. Other coordination modes: e) J. Breimair, C. Robl, W. Beck, *J. Organomet. Chem.* **1991**, *411*, 395–404; f) M.-C. Suen, G.-W Tseng, J.-D. Chen, T.-C. Keng, J.-C. Wang, *Chem. Commun.* **1999**, 1185–1186; g) F. A. Cotton, C. Lin, C. A. Murillo, *J. Am. Chem. Soc.* **2001**, *123*, 2670–2671. Examples of Mo(CO) fragments that contain carbonate bridges: h) E. Carmona, F. González, M. L. Poveda, J. M. Marin, J. L. Atwood, R. D. Rogers, *J. Am. Chem. Soc.* **1983**, *105*, 3365–3366; i) R. Alvarez, E. Carmona, A. Galindo, E. Gutiérrez, E. Marin, A. Monge, M. L. Poveda, C. Ruíz, J. M. Savariault, *Organometallics* **1989**, *8*, 2430–2439; j) R. Alvarez, J. L. Atwood, E. Carmona, P. Pérez, M. L. Poveda, R. D. Rogers, *Inorg. Chem.* **1991**, *30*, 1493–1499.

[31] D. J. Darensbourg, M. L. Meckfessel Jones, J. H. Reibenspies, *Inorg. Chem.* **1993**, *32*, 4675–4676.

[32] E. Hevia, J. Pérez, V. Riera, D. Miguel, *Chem. Commun.* **2002**, 1814–1815.

[33] E. Hevia, J. Pérez, V. Riera, D. Miguel, *Organometallics* **2003**, *22*, 257–263.

[34] J. March, *Advanced Organic Chemistry. Reactions, Mechanisms and Structure*, 4th ed, Wiley, **1992**, New York.

[35] Hydrolysis of metallacarbonate ester complexes to give carbonate complexes has previously been observed: a) T. Yoshida, T. Okano, Y. Ueda, S. Otsuka, *J. Am. Chem. Soc.* **1981**, *103*, 3411–3422; b) D. J. Darensbourg, K. M. Sanchez, J. H. Reibenspies, A. L. Rheingold, *J. Am. Chem. Soc.* **1989**, *111*, 7094–7103; c) R. D. Simpson, R. G. Bergman, *Organometallics* **1992**, *11*, 4306–4315.

[36] R. Alsfasser, S. Trofimenko, A. Looney, G. Parkin, H. Vahrenkamp, *Inorg. Chem.* **1991**, *30*, 4098–4100.

[37] D. H. Gibson, B. A. Sleaad, X. Yin, A. Vij, *Organometallics* **1998**, *17*, 2689–2691.

[38] M–OH bonds have been found to be stronger than M–OR bonds in related compounds, see reference [3].

[39] F. H. Allen, O. Kennard, D. G. Watson, L. Brammer, A. G. Orpen, R. Taylor, *J. Chem. Soc. Perkin Trans. 2* **1987**, 1-19.

[40] D. Morales, J. Pérez, L. Riera, V. Riera, D. Miguel, M. E. G. Mosquera, S. García-Granda, *Chem. Eur. J.* **2003**, *9*, 4132–4143.

[41] Examples of *trans*-dicarbonyl allyl Mo^{II} complexes: a) J. Pérez, V. Riera, A. Rodríguez, S. García-Granda, *Angew. Chem.* **2002**, *114*, 1485; *Angew. Chem. Int. Ed.* **2002**, *41*, 1427–1429; b) J. Pérez, V. Riera, A. Rodríguez, R. López, T. L. Sordo, S. García-Granda, E. García-Rodríguez, A. Galindo, *Organometallics* **2003**, *22*, 1540–1545. Examples of pseudo-octahedral allyl monocarbonyl complexes: c) K.-H. Yih, G.-H. Lee, S. L. Huang, Y. Wang, *Inorg. Chim. Acta* **2003**, *348*, 271–278; d) K.-H. Yih, G.-H. Lee, S.-L. Huang, Y. Wang, *Organometallics* **2002**, *21*, 5767–5774.

[42] However, formation of metallacycles that involve a CO group and a complex that contains a basic ligand (thiolato or phosphido) as a result of its reaction with DMAD has previously been observed: M. T. Ashby, J. H. Enemark, *Organometallics* **1987**, *6*, 1318–1323.

[43] a) J. Pérez, L. Riera, V. Riera, S. García-Granda, E. García-Rodríguez, *J. Am. Chem. Soc.* **2001**, *123*, 7469–7470; b) J. Pérez, L. Riera, V. Riera, S. García-Granda, E. García-Rodríguez, D. Miguel, *Organometallics* **2002**, *21*, 1622–1626; c) D. Morales, J. Pérez, L. Riera, V. Riera, D. Miguel, *Inorg. Chem.* **2002**, *41*, 4111–4113.

[44] J. Guerrero, O. E. Pino, E. Wolcan, M. R. Feliz, G. Ferraudi, S. A. Moya, *Organometallics* **2001**, *20*, 2842–2853.

[45] SAINT+. SAX area detector integration program. Version 6.02. Bruker AXS, Inc. Madison, WI, **1999**.

[46] Sheldrick, G. M. SHELXTL, An integrated system for solving, refining, and displaying crystal structures from diffraction data. Version 5.1. Bruker AXS, Inc. Madison, WI, **1998**.

[47] Sheldrick, G. M. SADABS, Empirical Absorption Correction Program. University of Göttingen: Göttingen, Germany, **1997**.

[48] P. T. Beurskens, G. Admiraal, G. Beurskens, W. P. Bosman, S. García-Granda, R. O. Gould, J. M. M. Smits, C. Smykalla, (**1992**).

The DIRDIF program system, Technical Report of the Crystallography Laboratory, University of Nijmegen, The Netherlands.
[49] G. M. Sheldrick, SHELXL-97, University of Göttingen, A computer program for refinement of crystal structures, **1997**.
[50] S. Parking, B. Moezzi, H. Hope, *J. Appl. Crystallogr.* **1995**, *28*, 53–56.
[51] M. Nardelli, *Comput. Chem.* **1983**, *7*, 95–98.
[52] A. L. Spek, PLATON, a multipurpose crystallo-graphic tool, Utrecht University, Utrecht, The Netherlands, **2001**.

Received: September 26, 2003 [F5577]